World Journal of Emergency Surgery

RESEARCH

Open Access

Prediction of infected pancreatic necrosis in patients with acute necrotizing pancreatitis based on ensemble machine learning model

Zefang Sun[1,2,3], Yan Fu[2,3,4], Jiarong Li[1,2,3], Baiqi Liu[1,2,3], Xiaoyue Hong[1,2,3], Chiayen Lin[1,2,3], Dingcheng Shen[1,2,3], Caihong Ning[1,2,3], Lu Chen[1,2,3], Xiaoping Yi[2,3,4*] and Gengwen Huang[1,2,3*]

Abstract

Background To study the value of ensemble machine learning (EL) model in the prediction of infected pancreatic necrosis (IPN) among patients with acute necrotizing pancreatitis (ANP).

Methods This study comprehensively analyzed 1073 acute necrotizing pancreatitis (ANP) patients admitted to Xiangya hospital from January 2011 to December 2023. The patients were divided into IPN group and sterile pancreatic necrosis (SPN) group based on IPN occurrence. All ANP patients were randomly divided into training dataset and validation dataset with a ratio of 7:3. The EL model was built by integrating multiple machine learning models (LASSO, random forest, and SVM). To verify the stability of the EL model, 78 ANP patients from the Third Xiangya hospital were included for external validation, and a Fagan nomogram was constructed to assess the posterior probability.

Results The EL model was constructed with 31 risk factors identified through LASSO regression. The prediction accuracy of the EL model in the training dataset was 92.6%. In the validation dataset, the prediction accuracy was 91.5%. Compared with the LR model, the EL model demonstrated higher AUC values (training dataset: 0.916 vs. 0.744; validation dataset: 0.919 vs. 0.742) and net benefit rate. The AUC of the EL model for predicting IPN within 7 days, 7–14 days, and after 14 days were 0.888, 0.906, and 0.901, respectively. In addition, the external validation results further indicated the accuracy of the EL model (AUC: 0.883). An EL model-based Fagan nomogram could be used to estimate the accuracy of IPN predictions.

Conclusion The EL model demonstrates superior predictive efficiency for IPN compared to the LR model, offering greater predictive value and potential clinical benefits. Furthermore, the EL model shows stable performance across different stages of IPN onset, enabling clinicians to make timely adjustments to treatment strategies and ultimately improve patient outcomes.

Trial registration The study is registered at www.researchregistry.com (Unique Identifying number: researchregistry10652).

*Correspondence:
Xiaoping Yi
yixiaoping@csu.edu.cn
Gengwen Huang
huanggengwen@csu.edu.cn

Full list of author information is available at the end of the article

Graphical Abstract

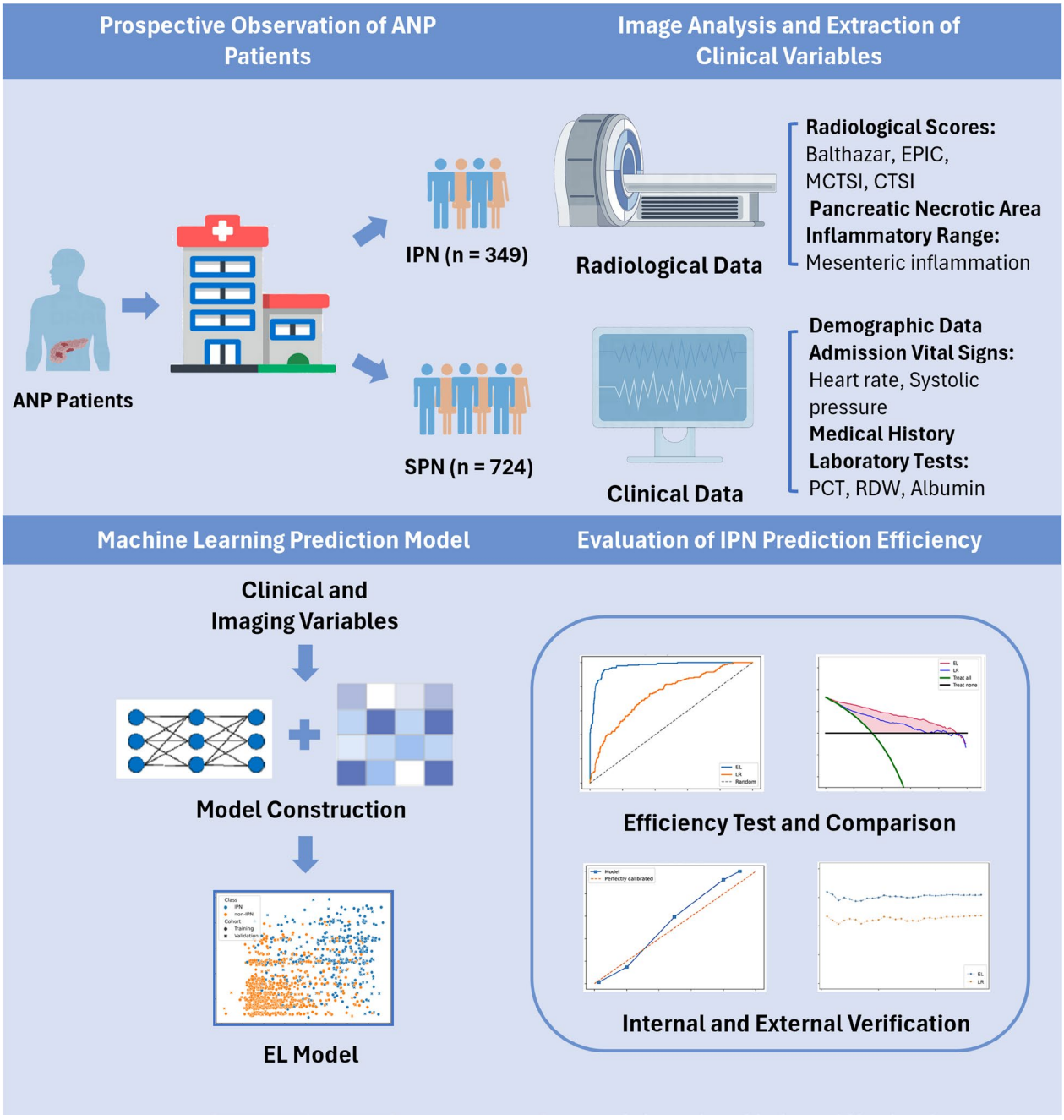

Keywords Acute necrotizing pancreatitis, Infected pancreatic necrosis, Ensemble machine learning, Risk factors, Precise prediction

Introduction

Acute necrotizing pancreatitis (ANP) is a severe form of acute pancreatitis (AP), characterized by necrosis of pancreatic parenchyma and/or surrounding tissues, with a mortality of 13%~22% [1–3]. One of the predominant causes of mortality in ANP patients is the infection of the necrotic tissue, also known as infected pancreatic necrosis (IPN). The mortality rate of IPN patients is as high as 32%~39% [4, 5]. Early prediction of IPN is critical for implementing preventive measures and initiating effective therapy, with the potential to improve clinical outcomes.

At present, accurate and early prediction of IPN is still very difficult. Various laboratory indicators and severity scoring systems have been investigated. Studies have shown that procalcitonin (PCT), hematocrit (HCT), interleukin-6 (IL-6), and gut microbiota could serve as predictive factors for IPN [6–9]. However, these individual indicators lacked predictive specificity and were infrequently used to diagnose IPN solely. Additionally, current radiological scoring systems mainly focused on predicting the severity of AP rather than accurately predicting the occurrence of IPN.

Given the difficulty in detecting the early onset of infections with a single biomarker, some studies have focused on using multiple markers to construct predictive models for early prediction. Most of the existing predictive models for IPN were developed using the logistic regression (LR) method, exhibiting considerable diversity in predictive performance [10, 11]. This variability makes it difficult for these models to be effectively applied in clinical practice. Therefore, it is imperative to develop a robust and accurate predictive model capable of effectively and accurately identifying IPN patients.

Machine learning (ML), a subset of artificial intelligence, represents an interdisciplinary domain encompassing statistics, computer science, and many other disciplines. With the application of efficient mathematical algorithms, ML aims to achieve precise prediction results by discerning complex relationships within the medical data [12]. Currently, ML has been gradually applied in the field of AP. In previous study, ML models have been developed to predict the severity of AP at early stage [13]. In our earlier study, a machine learning-based conditional survival model could accurately predict the prognosis of IPN patients [14]. However, due to the multitude and diverse characteristics of ML methods, it is challenging to evaluate which methods are best suited for specific medical scenarios. The ensemble machine learning (EL) approach can integrate the strengths of multiple methods to enhance predictive performance [15–17]. Nevertheless, the application of EL in predicting the occurrence of IPN remains scarce.

The aim of this study was to develop an EL based predictive model utilizing demographic information, laboratory metrics, and radiological scores from a large ANP cohort to accurately predict and identify patients with IPN, thereby assisting clinicians in timely antibiotic use and surgical intervention to improve IPN patient outcomes.

Methods and materials

Study cohort

Consecutive patients diagnosed with ANP from January 2011 to December 2023 in Xiangya hospital were prospective enrolled to construct the ANP cohort [14, 18–20] and underwent a post-hoc analysis. Patients with the history of chronic pancreatitis, pancreatitis due to pancreatic tumor, previous pancreatic surgery, and those with incomplete data were excluded. Finally, 1073 patients with ANP were included for prediction model construction, consisting of 349 patients with IPN and 724 patients with sterile pancreatic necrosis (SPN). A total of 78 ANP patients (including 27 IPN patients and 51 SPN patients) admitted to the Third Xiangya hospital between January 2023 and October 2024 were prospectively included for external validation to assess the stability of the EL model. The study was approved by the Ethics Committee of the study hospital and the collaborating hospital on December 2010, and supplementary registered on www.researchregistry.com (Unique Identifying number: researchregistry10652, https://researchregistry.knack.com/researchregistry#home/registrationdetails-/66d5c427667d8d02cd793b97/) on September 2024. The study was conducted according to STROCSS criteria [21]. Written informed consent was obtained from all participants or their legal representatives for publication of data.

Data collection and definition

After the completion of laboratory test and imaging examination, the clinical and imaging data of all admitted ANP patients were prospectively collected according to the electronic diagnosis and treatment system and medical records. The definition and classification of AP was based on the Revised Atlanta Classification (RAC) [22]. ANP was diagnosed as AP with non-enhancing areas of the pancreas on a contrast-enhanced computed tomography (CT) scan. Bacterial culture results from a peripancreatic specimen are used as a standard test for pancreatic infection [23]. IPN was defined as a positive culture of peri-pancreatic specimens obtained during the first necrosectomy or drainage. SPN was defined as a negative culture of peri-pancreatic specimens during the first surgical intervention or no signs of infection on discharge and follow-up period (90 days after discharge). Patients with ANP who met the above definition were diagnosed with IPN/SPN for subsequent modeling analysis.

In this study, specialized data collectors and analysts were employed to perform data collection and analysis without knowledge of patient group assignment to minimize the influence of human bias on the analysis results. The following data were collected from all eligible patients: (1) Demographic data, including age, gender, BMI, etiology, smoking history, alcohol consumption history, pregnancy history, chronic complications (hypertension, diabetes, and coronary diseases), temperature (T), heart rate (HR), blood pressure (BP). (2) Maximum values of the following clinical data within 3 days upon

admission: white blood cell count (WBC), red blood cell count (RBC), neutrophil count (N), lymphocyte count (L), eosinophil count (E), monocyte count (M), red blood cell volume distribution width (RDW), platelet specific volume (PST), mean platelet volume (MPV), serum albumin (A), serum globulin (G), alanine aminotransferase (ALT), aspartate aminotransferase (AST), C-reactive protein (CRP), PCT, blood urea nitrogen (BUN), creatinine (Cr), international normalized ratio (INR), and D-dimer. (3) Radiological data at admission: Balthazar score, CT severity index (CTSI) score, modified CT severity index (MCTSI) score and extra-pancreatic inflammation on CT (EPIC) score and its subitems (including pancreas morphology, pancreatic necrosis area, pleural effusion, ascitic fluid, portal vein (PV) and/or splenic vein (SV) thrombosis, mesenteric inflammation, retroperitoneal inflammation, etc.). In order to minimize the bias caused by the inclusion of ANP patients with different onset times, this study categorized patients into 3 subgroups (<7 days, 7–14 days, >14days) based on the onset time interval from diagnosis of AP to hospital admission. The potential risk factors of IPN and the predictive effectiveness of the prediction model were analyzed based on three subgroups.

CT image acquisition and scoring

All patients underwent CT scans using one of the three scanners: a 16-multi-detector CT (MDCT) (Brilliance 16, Philipps), a 64-MDCT (SOMATOM Definition, Siemens), or a 320-MDCT (Aquilion ONE, Toshiba Medical Systems) scanner. CT images were retrieved from the Picture Archiving and Communication System (PACS, Carestrem, Canada) and were reconstructed with an axial thickness of 1 mm.

CT images and scores for each patient were reviewed independently by two radiologists who were blinded to the patient information, including the radiological and clinicopathological data. Any disagreements were resolved in a panel format with one additional senior radiologist. The intra-class correlation coefficient (ICC) was used to evaluate the consistency and stability of radiological scores between the two radiologists. Generally, the ICC value greater than 0.75 is indicative of good agreement. The inter- and intra-observer reproducibility of the radiological parameters' evaluation was satisfactory in this study. The inter-observer ICC values of radiological scores evaluated by radiologist 1 and radiologist 2 in their first analysis ranged from 0.837 to 0.904. Subsequently, radiological data from 50 randomly selected patients were re-evaluated by two radiologists. The intra-observer ICC values for both evaluations performed by radiologist 1 ranged from 0.921 to 0.972 (Table S1). As a result, we used the evaluation results of radiologist 1 for the subsequent analysis.

Patient management protocols

All patients received standard treatment according to the latest international guidelines [24–26]. After admission, all patients were assessed by the multidisciplinary team, including pancreatic surgeons, intensive care units (ICU) physicians, gastroenterology physicians and radiologists. Patients with organ failure were treated in ICU with mechanical ventilation, continuous renal replacement therapy, vasoactive agents, and/or other measures. Surgical interventions were typically performed if there was suspicion of IPN, and were postponed for at least 3–4 weeks from the onset when possible. The step-up approaches consisting of percutaneous catheter drainage (PCD), minimal access retroperitoneal pancreatic necrosectomy (MARPN) and open pancreatic necrosectomy (OPN), was the preferred strategy for treating IPN. When sepsis could not be controlled with minimally invasive techniques or severe complications (such as massive bleeding or intestinal leakage) occurred, OPN would be the final resort of step-up approach. In contrast, OPN could be used as the initial surgical procedure to remove infected necrosis when there was no route for PCD or transluminal drainage. Detailed principles for the interventions of IPN could be found in our previous publications [18, 27, 28].

Predictive models

After all data collection and evaluation were completed, modeling analysis was conducted based on the obtained data. Two types of prediction models were developed. The EL model was constructed with ML algorithms, and multivariate LR method was utilized to build LR model. In previous studies, EL method has been successfully and efficiently applied in diagnosis, treatment response and prognosis prediction in a variety of diseases including IPN, renal cell carcinoma, ovarian cancer and colorectal cancer [14, 29–32].

For the EL algorithm, all data processing, data reduction, feature selection and model building were performed using MATLAB 2017a (The MathWorks, Inc, Natick, MA, USA). Multiple features from radiomic analysis, demographic and laboratory data were included in the ML analysis. The least absolute shrinkage and selection operator (LASSO) method was used for feature selection to reduce the collinearity between features. The cross-validation curve is used to evaluate the variation of penalty coefficient λ, and the minimum average error criterion is used to determine λ to obtain the number of non-zero features in the model (Figure S1, S2). The signature for each patient was calculated with the combination of the selected features by LASSO, weighted by respective coefficients. This composite score was termed as the Rad-score. Based on these selected features, the random forest (RF) method was used to establish another

Table 1 Cohort baseline data and laboratory results

	Onset time ≤ 7 days				7 days < Onset time ≤ 14 days				Onset time > 14 days			
	Total	**IPN**	**SPN**	**PValue**	**Total**	**IPN**	**SPN**	**PValue**	**Total**	**IPN**	**SPN**	**PValue**
Male proportion, n (%)	346 (67.4%)	75 (76.5%)	271 (65.3%)	0.033	119 (68.0%)	42 (62.7%)	77 (71.3%)	0.237	273 (70.9%)	136 (73.9%)	137 (68.2%)	0.215
Age, (IQR)	47 (37–57)	48 (37.25–55.75)	47 (37–57)	0.704	49 (42-56.5)	49 (38–54)	49 (43-59.25)	0.079	49 (39–57)	48 (38.75-55)	49 (39–60)	0.04
Temperature, (IQR)	37 (36.5–37.5)	37.05 (36.6-37.98)	36.9 (36.5–37.5)	0.019	37 (36.6–37.8)	37.1 (36.8–38.2)	37 (36.5–37.6)	0.057	37 (36.5–37.5)	37 (36.6–37.8)	36.8 (36.5–37.4)	0.012
Heart rate, (IQR)	**104 (90–120)**	**113 (100-123.75)**	**103 (90–117)**	**< 0.01**	**108 (94-123.5)**	**120 (102.5-133.5)**	**102 (90.75–118)**	**< 0.01**	**107 (92–120)**	**111 (100-123.25)**	**100 (88–117)**	**< 0.01**
Systolic pressure, (IQR)	**131 (115–149)**	**124 (109–148)**	**132 (115–149)**	**0.047**	**129 (111.5–147)**	**118 (108-142.5)**	**135.5 (121.75-149.25)**	**< 0.01**	**122 (110–139)**	**117.5 (106-135.25)**	**128 (112–140)**	**< 0.01**
BMI, (IQR)	25.39 (23.44–27.44)	25.31 (22.63–26.95)	25.51 (23.47–27.51)	0.343	24.46 (22.59–26.27)	23.8 (21.87–25.07)	24.91 (23.52–26.57)	< 0.01	24.01 (21.48–26.12)	23.17 (21-25.21)	24.65 (22.04–26.49)	< 0.01
Stomachache, n (%)	509 (99.2%)	98 (100.0%)	411 (99.0%)	0.331	174 (99.4%)	67 (100.0%)	107 (99.1%)	0.438	376 (97.7%)	183 (99.5%)	193 (96.0%)	0.026
Hypertension, n (%)	126 (24.6%)	22 (22.4%)	104 (25.1%)	0.59	44 (25.1%)	10 (14.9%)	34 (31.5%)	0.014	90 (23.4%)	37 (20.1%)	53 (26.4%)	0.148
Diabetes, n (%)	95 (18.5%)	11 (11.2%)	84 (20.2%)	0.039	33 (18.9%)	9 (13.4%)	24 (22.2%)	0.15	79 (20.5%)	35 (19.0%)	44 (21.9%)	0.487
Coronary_disease, n (%)	26 (5.1%)	0 (0%)	26 (6.3%)	0.011	9 (5.1%)	2 (3.0%)	7 (6.5%)	0.312	19 (4.9%)	4 (2.2%)	15 (7.5%)	0.017
Etiology, n (%)												
Biliary	212 (41.3%)	48 (49.0%)	164 (39.5%)	0.088	79 (45.1%)	33 (49.3%)	46 (42.6%)	0.392	185 (48.1%)	89 (48.4%)	96 (47.8%)	0.906
Alcohol	231 (45.0%)	34 (34.7%)	197 (47.5%)	0.022	60 (34.3%)	22 (32.8%)	38 (35.2%)	0.752	122 (31.7%)	55 (29.9%)	67 (33.3%)	0.469
Hypertriglyceridemia	21 (4.1%)	5 (5.1%)	16 (3.9%)	0.576	12 (6.9%)	4 (6.0%)	8 (7.4%)	0.718	14 (3.6%)	7 (3.8%)	7 (3.5%)	0.867
Others	49 (9.6%)	11 (11.2%)	38 (9.2%)	0.532	24 (13.7%)	8 (11.9%)	16 (14.8%)	0.594	64 (16.6%)	33 (17.9%)	31 (15.4%)	0.509
History of smoking, n (%)	161 (31.4%)	28 (28.6%)	133 (32.0%)	0.505	48 (27.4%)	19 (28.4%)	29 (26.9%)	0.83	123 (31.9%)	62 (33.7%)	61 (30.3%)	0.483
History of alcohol consumption, n (%)	174 (33.9%)	30 (30.6%)	144 (34.7%)	0.443	58 (33.1%)	22 (32.8%)	36 (33.3%)	0.947	130 (33.8%)	62 (33.7%)	68 (33.8%)	0.978
History of recent pregnancy, n (%)	22 (4.3%)	4 (4.1%)	18 (4.3%)	0.828	3 (1.7%)	2 (3.0%)	1 (0.9%)	0.312	4 (1.0%)	2 (1.1%)	2 (1.0%)	0.931

Table 1 (continued)

	Onset time ≤ 7 days				7 days < Onset time ≤ 14 days				Onset time > 14 days			
	Total	**IPN**	**SPN**	**PValue**	**Total**	**IPN**	**SPN**	**PValue**	**Total**	**IPN**	**SPN**	**PValue**
WBC, (IQR)	11.7 (8.6–15.5)	11.7 (7.95–14.97)	11.7 (8.85–15.75)	0.17	12.6 (9.15–18.1)	12.5 (8.55–17.95)	12.7 (9.28–18.12)	0.771	10.7 (6.7–15.4)	10.05 (6.3-15.43)	11.2 (7.3–15.4)	0.237
RBC, (IQR)	3.91 (3.27–4.49)	3.05 (2.65–4.11)	4.03 (3.54–4.5)	< 0.01	3.49 (2.91–4.05)	3.1 (2.75–3.71)	3.61 (2.97–4.15)	0.056	3.31 (2.81–4.15)	2.95 (2.64–3.39)	3.74 (3.12–4.43)	< 0.01
Neutrophil count, (IQR)	9.7 (6.6–13.3)	9.5 (6.12–12.88)	9.7 (6.85–13.45)	0.289	10.8 (7.25–16.35)	10.8 (6.9–16.6)	10.7 (7.83–16.12)	0.929	8.7 (5.1–13.2)	8.25 (4.6–13.1)	8.9 (5.4–13.4)	0.224
Lymphocyte count, (IQR)	0.9 (0.7–1.3)	0.9 (0.6–1.1)	1 (0.7–1.3)	0.08	0.9 (0.6–1.1)	0.8 (0.6–1.1)	0.9 (0.6–1.2)	0.607	0.9 (0.6–1.3)	0.9 (0.6–1.3)	0.9 (0.6–1.3)	0.387
Eosinophil count, (IQR)	0.07 (0-0.1)	0 (0-0.1)	0.09 (0-0.1)	0.067	0 (0-0.1)	0 (0-0.1)	0.1 (0-0.2)	0.031	0.02 (0-0.1)	0 (0-0.1)	0.1 (0-0.2)	< 0.01
RDW, (IQR)	**13.9 (13.2–14.9)**	**14.7 (13.7–15.9)**	**13.8 (13.1–14.7)**	**< 0.01**	**14.2 (13.4–15.3)**	**15.1 (14-15.85)**	**13.8 (13.1-14.72)**	**< 0.01**	**14.4 (13.4–15.7)**	**15 (14-16.3)**	**13.9 (13.1–14.9)**	**< 0.01**
PST, (IQR)	0.18 (0.13–0.23)	0.2 (0.13–0.29)	0.18 (0.13–0.22)	0.036	0.2 (0.14–0.3)	0.21 (0.13–0.3)	0.2 (0.14–0.28)	0.361	0.2 (0.15–0.26)	0.22 (0.15–0.29)	0.2 (0.14–0.26)	0.029
MPV, (IQR)	9.64 (8.71–10.9)	9.76 (8.71–10.5)	9.61 (8.71–10.93)	0.512	9.5 (8.73–10.75)	9.75 (8.79–10.84)	9.48 (8.67–10.7)	0.344	9.12 (8.38–10.39)	9.04 (8.28–10.1)	9.2 (8.45–10.42)	0.102
Albumin, (IQR)	**30.7 (27.7–34.1)**	**28.3 (25.63–30.4)**	**31.4 (28.4–34.9)**	**< 0.01**	**28.9 (25.7–33.1)**	**27.1 (24.1–30.7)**	**30.45 (27.23–33.78)**	**< 0.01**	**29.4 (25.9–33.2)**	**26.9 (24.5–30.4)**	**31.7 (28.5–35.1)**	**< 0.01**
Globulin, (IQR)	25.7 (22.5–28.5)	26.9 (23.92–31.7)	25.4 (22.2-27.85)	< 0.01	27.1 (22.95-32)	28.7 (22.85–34.3)	26.8 (23.12–30.02)	0.09	28.6 (24.2–33.7)	32.05 (27.37–35.73)	25.9 (22.2–30.6)	< 0.01
Ureanitrogen, (IQR)	5.62 (3.98–9.2)	6.93 (4.19–17.76)	5.52 (3.95–8.11)	< 0.01	6.86 (4.19–14.2)	9.08 (4.58–17.16)	5.91 (3.9-10.08)	0.022	5.32 (3.72–9.31)	5.74 (3.69–11.98)	5.15 (3.84–8.67)	0.456
INR, (IQR)	**1.14 (1.05–1.24)**	**1.21 (1.11–1.37)**	**1.12 (1.04–1.22)**	**< 0.01**	**1.15 (1.07–1.24)**	**1.17 (1.12–1.25)**	**1.11 (1.05–1.22)**	**< 0.01**	**1.17 (1.07–1.27)**	**1.22 (1.12–1.31)**	**1.12 (1.04–1.21)**	**< 0.01**
D-der, (IQR)	1.96 (1.04–3.79)	2.49 (1.6–6.96)	1.78 (0.95–3.36)	< 0.01	2.45 (1.48–5.66)	3.85 (1.71–6.88)	2.22 (1.42–4.06)	< 0.01	1.89 (0.95–4.05)	1.83 (0.99–3.86)	1.95 (0.88–4.08)	0.78
CRP, (IQR)	127.96 (44.5–221)	166.46 (83.05–299)	124 (40.49–205)	< 0.01	139.48 (91-223.76)	156 (91.05–279)	132.5 (91–216)	0.106	117 (44.75-196.63)	121.86 (60.5-187.75)	102 (30.11–203)	0.086

Table 1 (continued)

	Onset time ≤ 7 days				7 days < Onset time ≤ 14 days				Onset time > 14 days			
	Total	IPN	SPN	PValue	Total	IPN	SPN	PValue	Total	IPN	SPN	PValue
PCT, (IQR)	**1.38 (0.46–5.21)**	**3.34 (0.5-15.52)**	**1.23 (0.46–4.36)**	**<0.01**	**1.71 (0.52–6.09)**	**2.57 (1-6.78)**	**1.28 (0.46–4.88)**	**0.029**	**1.02 (0.34–3.94)**	**1.21 (0.3–4.23)**	**0.78 (0.39–3.39)**	**0.049**
Necrosis area > 30%, n (%)	**298 (58.1%)**	**87 (88.8%)**	**211 (50.8%)**	**<0.01**	**128 (73.1%)**	**59 (88.1%)**	**69 (63.9%)**	**<0.01**	**291 (75.6%)**	**160 (87.0%)**	**131 (65.2%)**	**<0.01**
Pleural effusion, n (%)	434 (84.6%)	88 (89.8%)	346 (83.4%)	0.114	159 (90.9%)	59 (88.1%)	100 (92.6%)	0.315	301 (78.2%)	153 (83.2%)	148 (73.6%)	0.024
Ascitic fluid, n (%)	446 (86.9%)	83 (84.7%)	363 (87.5%)	0.464	154 (88.0%)	56 (83.6%)	98 (90.7%)	0.159	309 (80.3%)	152 (82.6%)	157 (78.1%)	0.269
PV/SV thrombosis, n (%)	9 (1.8%)	0 (0.0%)	9 (2.2%)	0.142	4 (2.3%)	0 (0.0%)	4 (3.7%)	0.113	8 (2.1%)	1 (0.5%)	7 (3.5%)	0.044
Mesenteric inflammation, n (%)	**429 (83.6%)**	**87 (88.8%)**	**342 (82.4%)**	**0.046**	**150 (85.7%)**	**62 (92.5%)**	**88 (81.5%)**	**0.043**	**330 (85.7%)**	**168 (91.3%)**	**162 (80.6%)**	**<0.01**
Balthazar score, (IQR)	3 (3–4)	4 (3–4)	3 (2–3)	0.056	4 (3–4)	4 (3–4)	3 (2–4)	0.067	3 (3–4)	4 (3–4)	3 (3–4)	0.071
EPIC score, (IQR)	6 (4–7)	6.5 (5–7)	6 (4–7)	0.308	7 (5–7)	7 (5–7)	6 (4.75-7)	0.103	6 (3–7)	7 (5–7)	5 (3–7)	<0.01
MCTSI score, (IQR)	**6 (6–8)**	**8 (6–10)**	**6 (4–8)**	**<0.01**	**8 (6–10)**	**10 (6–10)**	**8 (6–8)**	**<0.01**	**8 (6–10)**	**10 (6–10)**	**8 (6–10)**	**<0.01**
CTSI score, (IQR)	**4 (3–6)**	**7 (4–10)**	**4 (3–6)**	**<0.01**	**6 (4–8)**	**8 (4.5–10)**	**6 (4–6)**	**<0.01**	**6 (4–8)**	**8 (4–10)**	**6 (3–8)**	**<0.01**

classification model and to generate the RF-score. Subsequently, according to the Rad-score and RF-score, the combined classification model was established by the support vector machine (SVM) method (SVM-score). Three additional SVM scores were generated based on the demographic, laboratory and image scoring features. The final EL model was built using the SVM algorithm with the four types of SVM-scores that have been generated by the proceeding steps. Its inputs were SVM scores of each data type, which was treated as weak classifier. Since the SVM scores were derived from different data types and independently obtained by various weak regressors, combining the scores in a two-dimensional plane using SVM produced better results than regressing each score individually. Finally, the regressed scores could be binarized for further prediction. In the whole process, risk factors identified by LASSO were also incorporated into the construction of the LR model. To minimize the loss of clinically important features, all relevant risk factors were included. Generalized linear models (GLM) were employed to construct the LR models.

To evaluate the performance of the models, the patients were randomly divided into training cohort and validation cohort with a ratio of 7:3. The models were developed in the training cohort and validated in the validation cohort. The classification efficiency in the training and validation cohort was calculated, and the receiver operating characteristic (ROC) curves, calibration curves (Hosmer-Lemeshow test) and brier score were used to evaluate the models. The clinical benefit rate of the models was assessed through decision curve analysis in the validation cohort. Additionally, external data from the collaborating hospital were used for external validation to assess the model's stability.

Statistical analysis

Data analysis and visualization were performed using R and Python software. The Shapiro-Wilk test was applied to assess the normality of the data. Continuous data with a normal distribution are presented as mean (standard deviation, SD) and were analyzed using Student's t-test, while continuous data with a non-normal distribution are presented as median (interquartile range, IQR) and analyzed using the Mann-Whitney U test. Categorical variables were compared using the Pearson chi-square test or Fisher's exact test. Internal validation was conducted using 1000 bootstrap resampling, and 95% confidence intervals (CIs) were calculated. The overall predictive efficiency of the EL models was evaluated by AUC, sensitivity, specificity, and Matthews correlation coefficient (MCC). The Delong test was utilized to compare the significant differences of AUC between different predictive models [33]. The positive and negative likelihood ratio was calculated and the Fagan's nomogram was

constructed to assist clinicians in evaluating the posterior probability when using EL models to predict IPN [34]. A *P*-value < 0.05 was considered statistically significant.

Results

Patient characteristics

A total of 1073 patients with ANP were included for model construction. There were 349 patients defined as IPN and 724 patients defined as SPN. To minimize data bias caused by differences in the time of onset, ANP patients were divided into three subgroups based on time of onset (< 7 days, 7–14 days, > 14days). The demographic and clinical characteristics of the cohort were summarized in Table 1. ANP patients recruited from the collaborating hospital served as an external cohort. The demographic and clinical characteristics of the external cohort are summarized in Table S2. There were significant differences in HR, PCT, albumin level, RDW, pancreatic necrosis area > 30%, mesenteric inflammation, MCTSI score and CTSI score among the three subgroups. Compared with the SPN group, the IPN group patients had faster HR, higher PCT, higher rates of pancreatic necrosis area > 30% and mesenteric inflammation. The MCTSI score and CTSI score of IPN group were also higher than SPN group. In addition, the IPN group had lower albumin and higher RDW compared to SPN group, indicating poorer nutritional status and baseline condition. The external validation data further confirmed these results (Table S2).

Construction of prediction models

The patients were randomly assigned to the training cohort ($n = 751$) and validation cohort ($n = 322$) with a ratio of 7:3. Details of the flowchart for building the classification model were shown in Fig. 1. The LASSO method integrated demographic information, laboratory metrics, and radiological parameters to select features for building predictive models. After dimensionality reduction, 7 demographic features (including age, male proportion, T, HR, SB, BMI, and etiology), 14 laboratory metrics (including WBC, RBC, N, L, RDW, PST, MPV, A, G, BUN, Cr, INR, CRP, and PCT), and 10 radiological parameters (including pancreas morphology, pancreatic necrosis area, pleural effusion, ascitic fluid, mesenteric inflammation, retroperitoneal inflammation, Balthazar score, EPIC score, MCTSI score, and CTSI score) were selected. According to the fitting scores of the selected features, the EL model was integrated by using SVM method. The results suggested that the EL model had a significantly higher predictive score for IPN patients compared to SPN patients, and was able to effectively differentiate between IPN and SPN patients (Fig. 2A). The

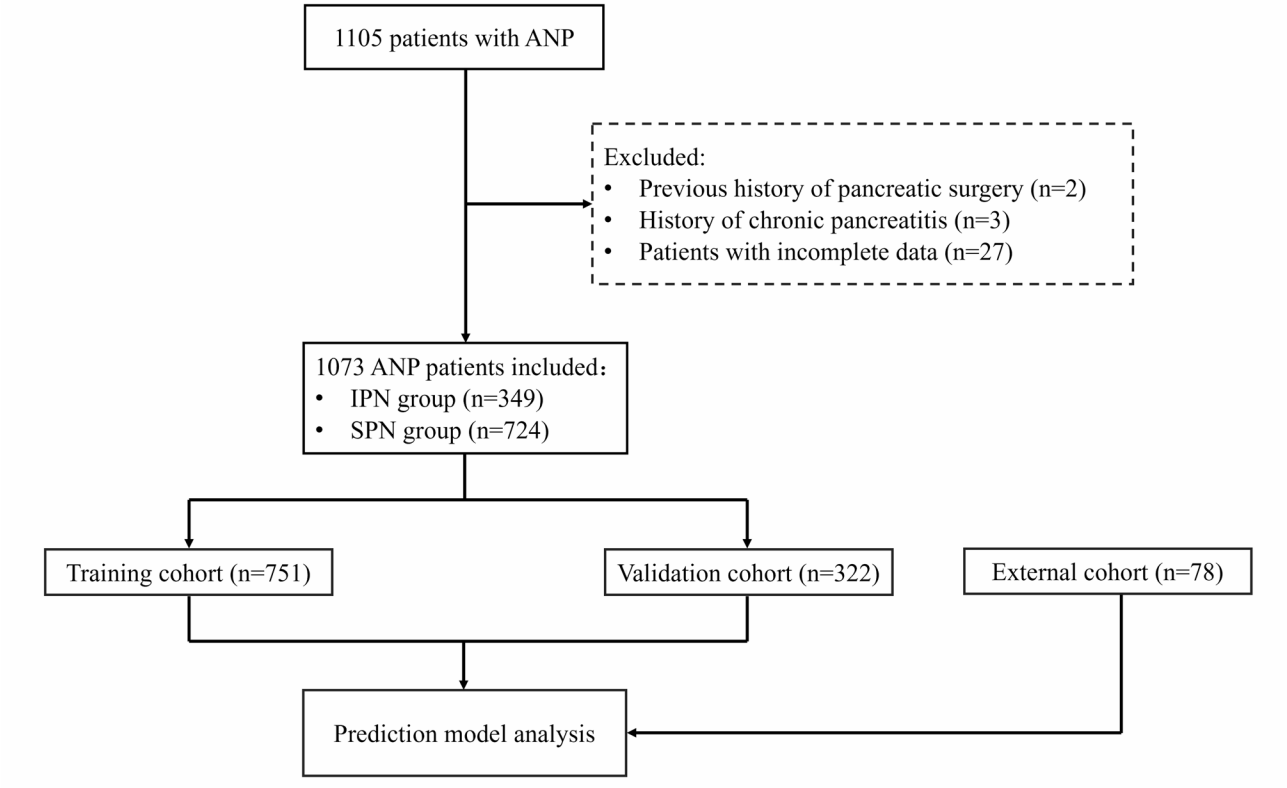

Fig. 1 Study cohort grouping and exclusion criteria

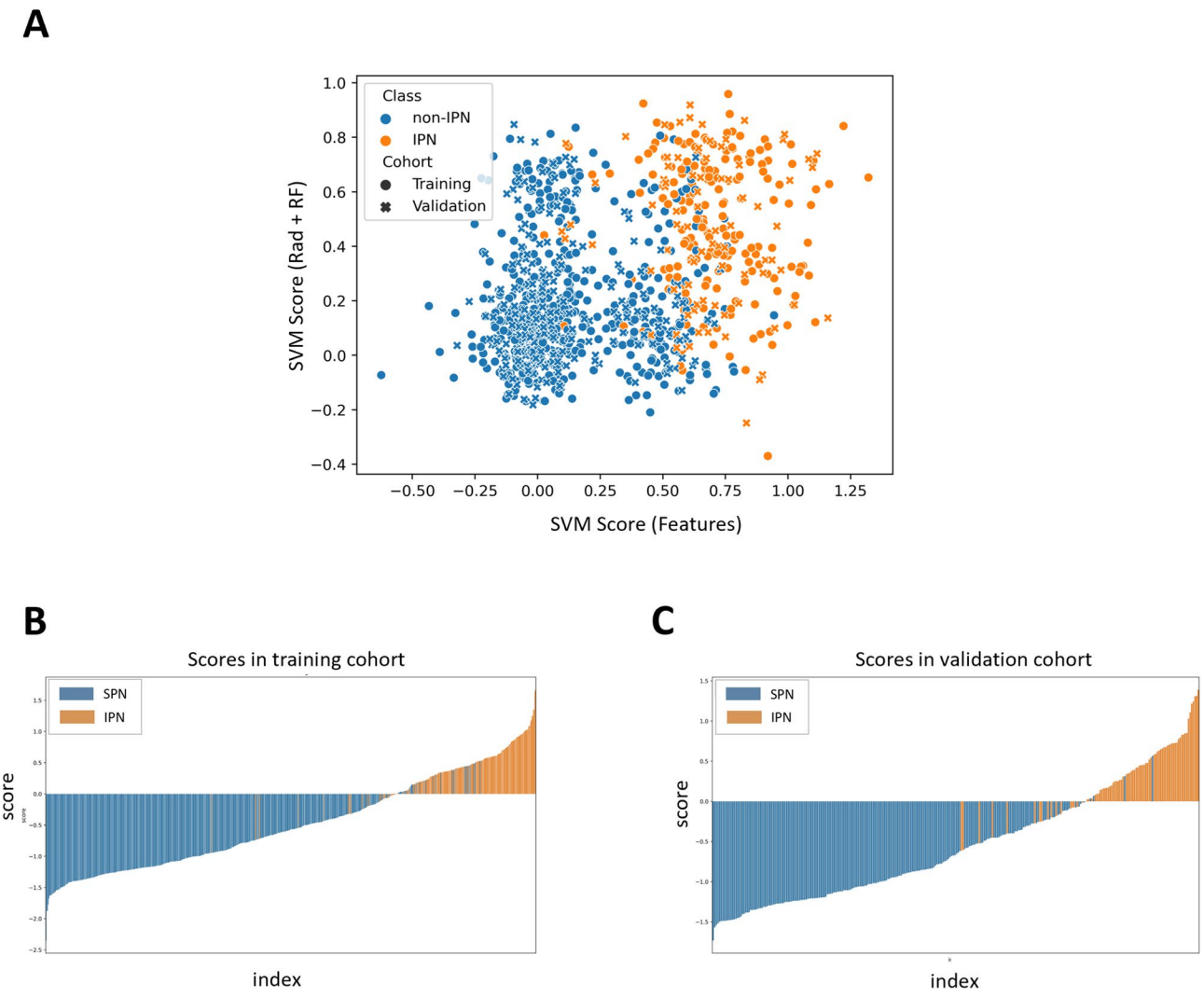

Fig. 2 Model construction and classification effect. (**A**) The scatterplot showed that the SVM score (combining Rad and RF scores) and SVM score (integrated clinical and radiological features) obtained by EL model can distinguish IPN patients from SPN patients; (**B**) Predicted scores of IPN and SPN patients obtained by EL model in the training dataset; (**C**) Predicted scores of IPN and SPN patients obtained by EL model in the validation dataset

prediction accuracy for IPN in the training cohort using the EL model was 92.6%. In the validation cohort, the prediction accuracy was 91.5% (Fig. 2B and C).

Model performance

The EL model demonstrated robust performance in training cohort (AUC: 0.916) and validation cohort (AUC: 0.919). Compared with the EL model, the AUC of LR model in the training cohort and validation cohort are 0.744 and 0.742, respectively (Fig. 3A and B). Based on the comprehensive results of AUC, sensitivity, specificity, and MCC, the EL model significantly was outperformed the LR model in predicting IPN (Table S3). The results of the Delong test indicated that there existed a significant difference in the AUC of the two prediction models (Table S4). In both the training and validation cohorts, the calibration curve of the EL model showed good consistency between prediction and clinical diagnosis (Fig. 3C and D). The C-index of the EL model was 0.873 in the training cohort and 0.868 in the validation cohort. The Brier scores were 0.057 and 0.060, respectively. These results suggested that the EL model demonstrated better prediction efficiency (Table S5). The external validation results further confirmed the predictive performance of the EL model. The AUC of the EL model in predicting external data was 0.883, still outperforming the LR model (Fig. 4D). The prior probability of the cohort was calculated according to the number of IPN patients in the training dataset and validation dataset, and the posterior probability could be estimated by combining the likelihood ratio. It can help clinicians effectively assess the true likelihood of IPN in ANP patients (Fig. 5). In addition, the decision curve of the prediction model indicated

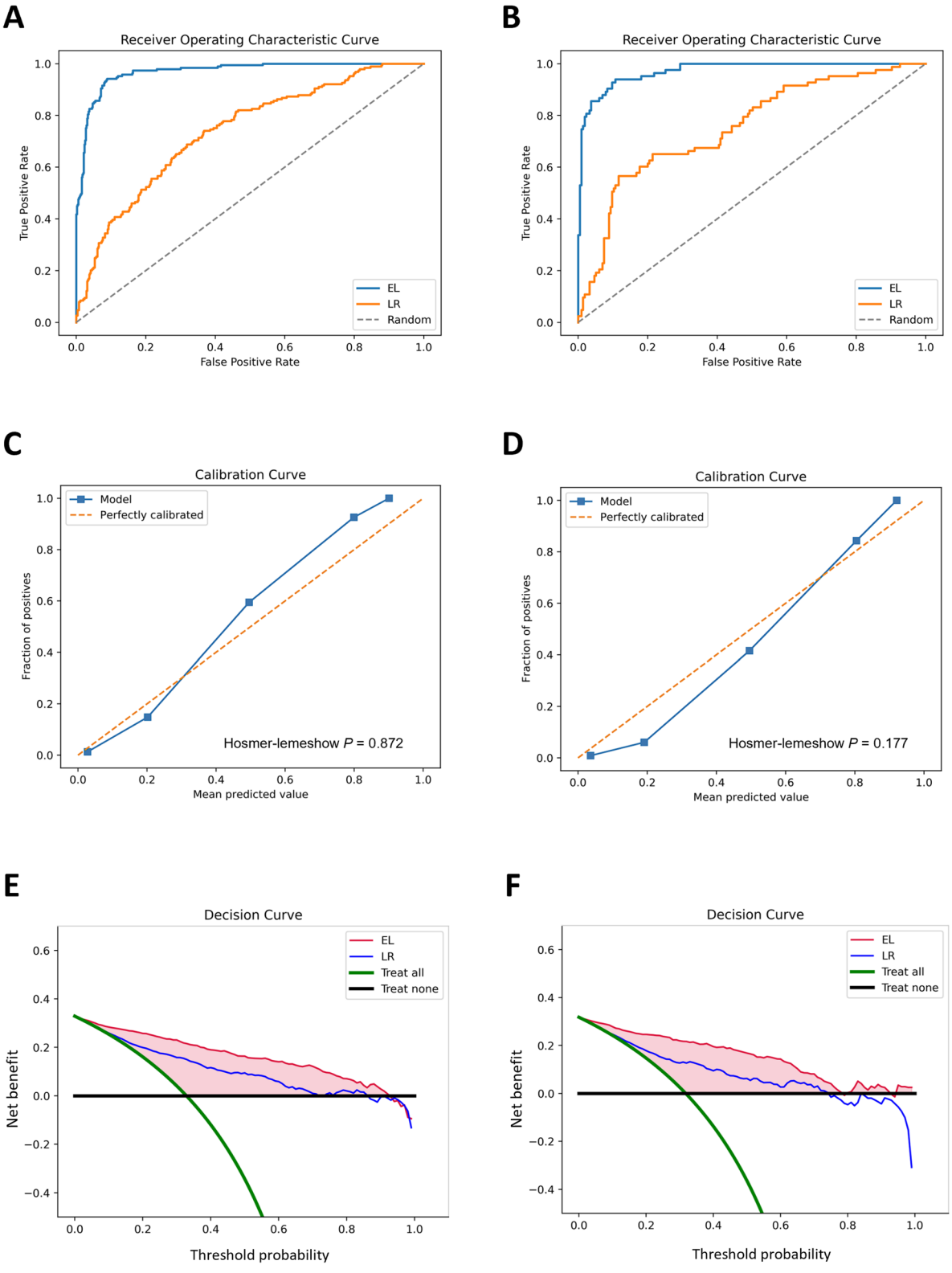

Fig. 3 Model efficiency comparison and internal verification. (**A**) AUC of EL model and LR model in training dataset; (**B**) AUC of EL model and LR model in validation dataset; (**C**) Calibration curve of EL model in training dataset; (**D**) Calibration curve of EL model in validation dataset. (**E**) Decision curve of EL model and LR model in training dataset; (**F**) Decision curve of EL model in validation dataset

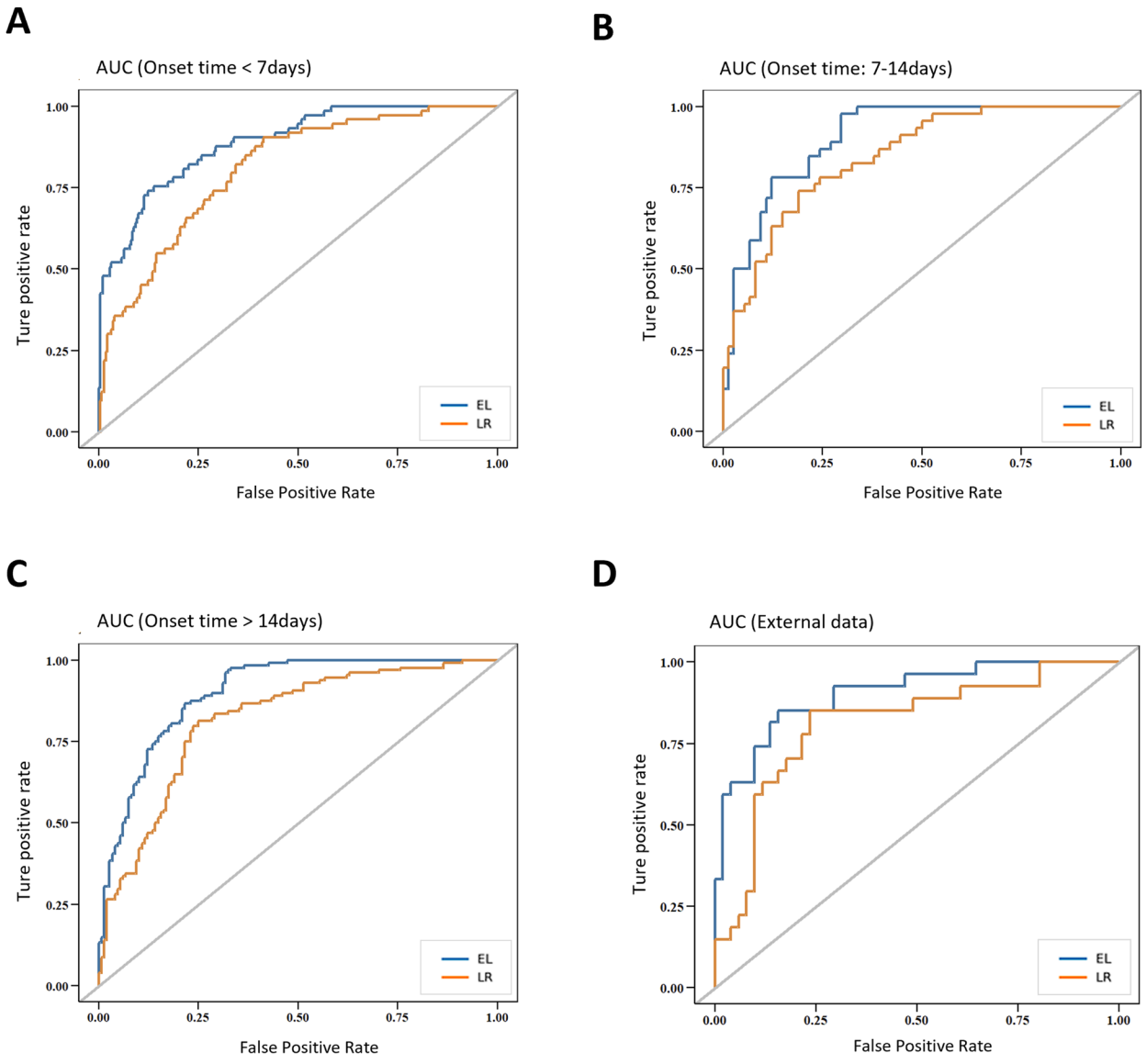

Fig. 4 Subgroup analysis of EL model with different onset time. (**A**) AUC of EL model and LR model (onset time < 7 days); (**B**) AUC of EL model and LR model (onset time: 7–14 days); (**C**) AUC of EL model and LR model (onset time > 14 days); (**D**) AUC of EL model and LR model for external data

that the EL model resulted in more clinical benefits than the LR model (Fig. 3E and F).

Prediction performance at different stages

To further assess the efficacy of EL model in predicting IPN at different stages, patients were divided into three subgroups according to the onset time (< 7 days, 7–14 days, > 14days). The results showed that the AUC of the EL model was higher than the LR model in all three subgroups (Fig. 4A, B and C), and Delong test results suggested that AUC of EL model and LR model in different subgroups was significantly different (Table S4). Overall, the AUC for IPN patients with different onset times (1–28 days) predicted by the EL model remained around 0.9, demonstrating robust and stable predictive efficacy (Figure S3).

Discussion

In this study, an EL model that integrated demographic characteristics, clinical laboratory variables, and radiological scoring data was developed to predict the occurrence of IPN. The results demonstrated that the EL model outperformed the traditional LR model in predicting IPN. This enhanced predictive capability facilitated earlier diagnosis of IPN, allowing for more effective guidance of subsequent treatment plans. To our knowledge,

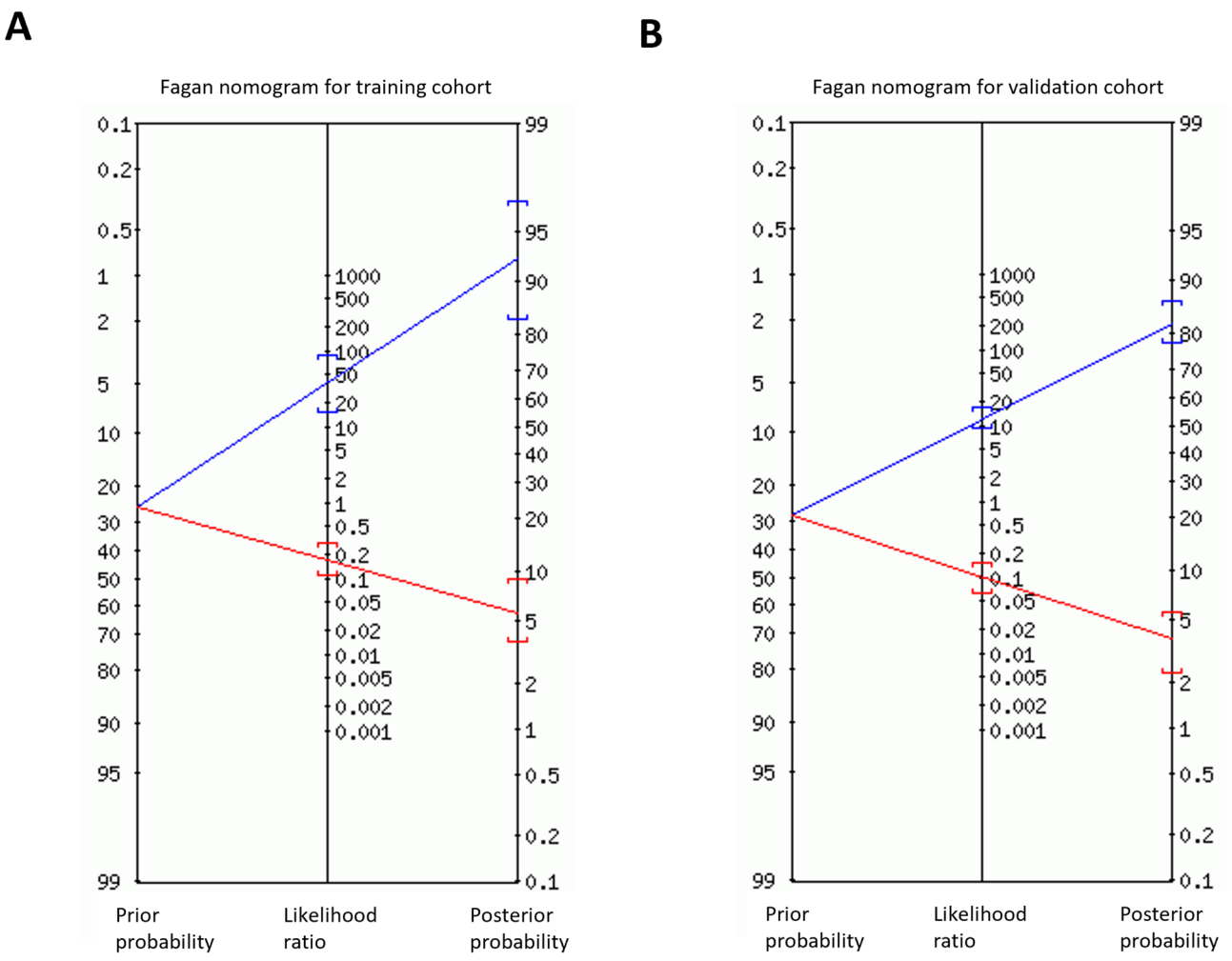

Fig. 5 Fagan nomogram for predictive model. (**A**) Fagan nomogram for predictive model in training dataset. The blue line represents a positive likelihood ratio and the red line represents a negative likelihood ratio; (**B**) Fagan nomogram for predictive model in validation dataset. The blue line represents a positive likelihood ratio and the red line represents a negative likelihood ratio

this is the first study to use an ensemble ML model combining clinical and radiological data to predict the occurrence of IPN.

In the past, the mortality in ANP patients exhibited two distinct peaks. The first peak (< 2 weeks) was characterized by multiple organ failure (MOF), and the second peak (> 2 weeks) was caused by complications such as IPN [35]. Recent advancements in critical care have significantly reduced early mortality due to MOF in patients with ANP. Therefore, effective treatment of IPN became the most crucial factor to improve the survival rate. In recent years, multiple surgical and endoscopic interventions have been incorporated into clinical practice to remove the infected necrotic tissues and control the source of infection, effectively reducing the mortality rate of IPN patients [36–38]. However, there were still many unresolved issues, the most important of which was the early diagnosis of IPN. The current diagnostic techniques, scoring systems and biomarkers for the early prediction of IPN remained unsatisfactory and warranted further study. In the present study, 7 demographic features, 14 laboratory metrics, and 10 radiological parameters were selected by LASSO method. Based on these risk factors, an ensemble machine learning based model was constructed for the accurate prediction of IPN.

The EL model incorporated a series of laboratory parameters, including HR, albumin levels, and PCT, which have been suggested to be associated with IPN [7, 11, 39, 40]. Nevertheless, Michael et al. found that the AUC for albumin in predicting pancreatic infection was only 0.71 [41]. Rau et al. observed that while the negative predictive value of PCT for predicting IPN was 0.93, its positive predictive value was only 0.52 [42]. The limited predictive performance of these laboratory metrics was not surprising. Local pancreatic infection often accompanied systemic inflammatory responses (SIRS), leading to alterations of these laboratory parameters. Therefore, individual parameters have limited performance in

predicting IPN and comprehensive assessment of various laboratory parameters was necessary.

Through LASSO selection, the most relevant risk factors for IPN were included in the construction of the EL model. In this model, in addition to the risk factors previously used to predict IPN occurrence, RDW was found to be associated with IPN. Previous studies have highlighted the correlation between RDW and the severity of sepsis and severe acute pancreatitis [43, 44]. Additionally, research by Murat et al. also suggested potential association between elevated RDW and *Acinetobacter baumanni* infection in ICU [45]. On this basis, the present study is the first to report an association between RDW and the occurrence of IPN, and to incorporate RDW into the prediction model of IPN.

The radiological score was considered closely related with the prognosis of ANP patients, but its performance in predicting the occurrence of IPN was limited [10, 46, 47]. Indeed, risk factors such as pancreatic morphology and the area of necrosis have been demonstrated to be associated to IPN [48, 49]. This suggested that adjustments to the calculation parameters of key subitems within the radiological score were necessary when predicting pancreatic infection. Through ML methods, various radiological scores and important subitems were simultaneously included into the EL model, and reassigned coefficients to better suit the prediction of IPN. Consistent with our hypothesis, the results of feature screening indicated that parameters within radiological scores, including pancreatic morphology, pancreatic necrosis area, and mesenteric inflammation, could contribute to predicting the occurrence of IPN. Compared to using only the total score, incorporating these key subitems enhanced the predictive efficiency of the EL model. A potential explanation was that extensive pancreatic necrosis and mesenteric inflammation might promote infection by altering the permeability of the intestinal wall, allowing bacteria from the intestine to enter the peripancreatic area and bloodstream [50–52]. This hypothesis warrants further profound mechanism analysis to facilitate the understanding of radiological data in IPN.

The results of this study demonstrated that the EL model outperformed the LR model in predicting the occurrence of IPN. Consistent with prior research, despite the inclusion of partially inconsistent factors, the predictive efficiency of the LR model remained between 0.7 and 0.8 [7, 11, 48, 53]. In contrast, the predictive efficiency of the EL model reached up to 0.9, significantly improving the accuracy of IPN prediction. This result was further validated in the external data. In the result of external validation, the AUC of EL model remained stable and outperformed the LR model (AUC: 0.883 vs. 0.811). These results suggest that the EL model could provide better auxiliary guidance for the diagnosis of IPN. Consistent with present study, Lan et al. utilized ML model to predict the timing of surgical intervention for ANP patients, achieving a diagnostic efficiency of 0.9 [54], which exemplified the superiority of ML algorithms. Previous studies have highlighted that SVM and LASSO methods are superior to LR methods in predictive modeling due to the non-linear nature of medical predictions [55, 56]. During the feature selection, LR methods typically choose limited number of features to avoid overfitting, which might inadvertently discard clinically significant features. In contrast, ensemble machine learning algorithms reduced the risk of losing valuable features by combining them into a single factor, which was then used as a unified feature set for modeling, resulting in improved model performance. Currently, most IPN related studies have limited sample sizes, leading to unstable predictive performance of the models. This could increase cohort heterogeneity, introduce significant bias in prediction outcomes, and potentially contribute to the overuse and misuse of antibiotics in patients with ANP. The judicious application of ML methods could lead to the development of more precise models, mitigating these issues and providing greater clinical benefits. Furthermore, the ensemble pattern of ML takes into account the opinions of multiple classifiers rather than one, enhancing the model's anti-noise and generalization capabilities, as well as increasing the reliability of clinical predictive results. In addition, the Fagan nomograms based on machine learning results could assist clinicians accurately assess the posterior probability of IPN occurrence, thereby guiding antibiotic use and surgical intervention more precisely.

In this study, patients with ANP admitted at different onset times were included in the cohort for model training. This inclusion strategy was influenced by the fact that the research institution, one of the largest pancreatitis treatment centers in China, receives ANP patients from all over the country, with varying onset times upon admission. Therefore, the ability to widely identify and predict IPN patients with different onset times have significant medical value. At the same time, early prediction of the occurrence of IPN was important equally for subsequent treatment decisions. Consequently, we assessed the predictive performance of the EL model across different onset time categories (< 7 days, 7–14 days, > 14days). The results indicated that the prediction performance of EL model for IPN patients with different onset times remained consistently at 0.9, demonstrating the model's ability to accurately and early predict IPN.

The current study has several limitations. Firstly, since most IPN patients were admitted through referrals, it was possible that early treatment data for many patients might be missed during the referral process. Secondly,

although the EL model was developed using a large ANP cohort and underwent external validation, the extended timeframe of the study cohort introduces potential historical bias due to evolving diagnostic criteria and treatment protocols. Furthermore, the limited external data, sourced solely from the same province, may impact on the generalizability of the EL model. Further validation of larger external datasets is still needed to confirm its stability. Thirdly, a small number of ANP patients who lacked evidence of pathogenic microorganisms from peri-pancreatic specimens due to death prior to surgical intervention were excluded from this study. These patients were critically ill, and infection may have been a significant contributing factor to their death. Fourth, while EL models provided valuable insights, the current EL model still lacks explainability and uses only a single ensemble ML method without comparisons, which can introduce bias. Therefore, future research directions should prioritize model optimization and conduct larger-scale, multicenter randomized controlled trials to validate our findings and comprehensively address these limitations.

In summary, a robust EL model by integrating clinical and radiological data of ANP patients was developed to predict the occurrence of IPN. The predictive performance of the EL model surpassed the LR model in both internal and external validation and demonstrated consistent predictive efficacy at different stages. As a result, the EL model can offer reliable assistance for the diagnosis of IPN and subsequent endoscopic or surgical interventions.

Conclusion

In this study, we used ensemble machine learning method to construct an EL model based on 31 IPN related risk factors, which can accurately predict the risk of IPN in ANP patients at different onset times. Moreover, EL model has more advantages in IPN prediction than traditional LR model, and the Fagan nomogram constructed based on the EL model can help clinicians evaluate the posterior probability of IPN. To our knowledge, this study represents one of the largest prospective cohorts in the existing literature to use ensemble ML methods for predicting IPN, which could help clinicians make early adjustments to treatment strategies and ultimately improve outcomes for IPN patients.

Abbreviations

AP	Acute pancreatitis
ANP	Acute necrotizing pancreatitis
IPN	Infected pancreatic necrosis
SPN	Sterile pancreatic necrosis
LR	Logistic regression
ML	Machine learning
RAC	The Revised Atlanta Classification
PCD	Percutaneous catheter drainage
MARPN	Minimal access retroperitoneal pancreatic necrosectomy
OPN	Open pancreatic necrosectomy
EL	Ensemble machine learning
CTSI	CT severity index score
MCTSI	Modified CT severity index score
EPIC	Extra-pancreatic inflammation on CT

Supplementary Information

The online version contains supplementary material available at https://doi.org/10.1186/s13017-025-00642-2.

Supplementary Material 1

Supplementary Material 2

Supplementary Material 3

Supplementary Material 4

Supplementary Material 5

Supplementary Material 6

Supplementary Material 7

Supplementary Material 8

Acknowledgements

Acknowledgements to Jie Xiao (Third Xiangya Hospital) and Di Wu (Third Xiangya Hospital) for supporting this study in the construction of external cohort and clinical data collection.

Author contributions

Zefang Sun: Conceptualization, Project administration, Writing - Original Draft, Writing - Review & Editing. Yan Fu: Methodology, Formal analysis, Visualization, Writing - Review & Editing. Jiarong Li: Data curation, Writing - Review & Editing. Baiqi Liu: Data curation, Resources, Writing - Review & Editing. Xiaoyue Hong: Data curation, Writing - Review & Editing. Chiayen Lin: Data curation, Writing - Review & Editing. Dingcheng Shen: Data curation, Writing - Review & Editing. Caihong Ning: Data curation, Writing - Review & Editing. Lu Chen: Supervision, Writing - Review & Editing. Xiaoping Yi: Conceptualization, Supervision, Resources, Writing - Review & Editing, Project administration. Gengwen Huang: Conceptualization, Supervision, Resources, Funding acquisition, Writing - Review & Editing, Project administration. All authors approved the final version of the manuscript.

Funding

This work was supported by the Project Program of National Clinical Research Center for Geriatric Disorders (Xiangya Hospital, Grant No. 2021LNJJ19).

Data availability

The datasets used and/or analyzed for the present study are available from the corresponding author (Gengwen Huang, huanggengwen@csu.edu.cn) on reasonable request.

Declarations

Ethics approval and consent to participate

For the clinical study protocol, it was set in compliance with Helsinki Declaration and was approved by the Ethics Committee of Xiangya hospital on 5 December 2010 (reference: 201012072). Written informed consent was obtained from all participants or their legal representatives before enrollment.

Consent for publication

Written informed consent was obtained from all participants or their legal representatives for publication of data.

Competing interests

The authors declare no competing interests.

Author details
[1]Division of Pancreatic Surgery, Department of General Surgery, Xiangya Hospital, Central South University, 87 Xiangya Rd, Changsha 410008, Hunan Province, China
[2]National Clinical Research Center for Geriatric Disorders, Xiangya Hospital, Central South University, Changsha 410008, Hunan Province, China
[3]FuRong Laboratory, Changsha 410078, Hunan Province, China
[4]Department of Radiology, Xiangya Hospital, Central South University, 87 Xiangya Rd, Changsha 410008, Hunan Province, China

Received: 14 April 2025 / Accepted: 31 July 2025
Published online: 07 August 2025

References

1. Schepers N, Bakker O, Besselink M, et al. Impact of characteristics of organ failure and infected necrosis on mortality in necrotising pancreatitis. Gut. 2019;68(6):1044–51. https://doi.org/10.1136/gutjnl-2017-314657.
2. Guo Q, Li A, Xia Q, et al. The role of organ failure and infection in necrotizing pancreatitis: a prospective study. Ann Surg. 2014;259(6):1201–7. https://doi.org/10.1097/SLA.0000000000000264.
3. Garg P, Madan K, Pande G, et al. Association of extent and infection of pancreatic necrosis with organ failure and death in acute necrotizing pancreatitis. Clin Gastroenterol Hepatol. 2005;3(2):159–66. https://doi.org/10.1016/s1542-3565(04)00665-2.
4. Bugiantella W, Rondelli F, Boni M, et al. Necrotizing pancreatitis: A review of the interventions. Int J Surg. 2016;28(Suppl 1):S163–171. https://doi.org/10.1016/j.ijsu.2015.12.038.
5. Petrov MS, Shanbhag S, Chakraborty M, Phillips AR, Windsor JA. Organ failure and infection of pancreatic necrosis as determinants of mortality in patients with acute pancreatitis. Gastroenterology. 2010;139(3):813–20. https://doi.org/10.1053/j.gastro.2010.06.010.
6. Mofidi R, Suttie SA, Patil PV, Ogston S, Parks RW. The value of procalcitonin at predicting the severity of acute pancreatitis and development of infected pancreatic necrosis: systematic review. Surgery. 2009;146(1):72–81. https://doi.org/10.1016/j.surg.2009.02.013.
7. Chen HZ, Ji L, Li L, et al. Early prediction of infected pancreatic necrosis secondary to necrotizing pancreatitis. Medicine (Baltimore). 2017;96(30):e7487. https://doi.org/10.1097/MD.0000000000007487.
8. Li J, Chen Z, Li L, et al. Interleukin-6 is better than C-reactive protein for the prediction of infected pancreatic necrosis and mortality in patients with acute pancreatitis. Front Cell Infect Microbiol. 2022;12:933221. https://doi.org/10.3389/fcimb.2022.933221.
9. Zou M, Yang Z, Fan Y, et al. Gut microbiota on admission as predictive biomarker for acute necrotizing pancreatitis. Front Immunol. 2022;13:988326. https://doi.org/10.3389/fimmu.2022.988326.
10. Zeng YB, Zhan XB, Guo XR, et al. Risk factors for pancreatic infection in patients with severe acute pancreatitis: an analysis of 163 cases. J Dig Dis. 2014;15(7):377–85. https://doi.org/10.1111/1751-2980.12150.
11. Wiese ML, Urban S, von Rheinbaben S, et al. Identification of early predictors for infected necrosis in acute pancreatitis. BMC Gastroenterol. 2022;3(1):405. https://doi.org/10.1186/s12876-022-02490-9.
12. Deo RC. Machine learning in medicine. Circulation. 2015;17(20):1920–30. https://doi.org/10.1161/CIRCULATIONAHA.115.001593.
13. Kui B, Pinter J, Molontay R, et al. EASY-APP: an artificial intelligence model and application for early and easy prediction of severity in acute pancreatitis. Clin Transl Med. 2022;12(6):e842. https://doi.org/10.1002/ctm2.842.
14. Ning C, Ouyang H, Shen D, et al. Prediction of survival in patients with infected pancreatic necrosis: a prospective cohort study. Int J Surg. 2023;110(2):777–87. https://doi.org/10.1097/JS9.0000000000000844.
15. Muhlestein WE, Akagi DS, McManus AR, Chambless LB. Machine learning ensemble models predict total charges and drivers of cost for transsphenoidal surgery for pituitary tumor. J Neurosurg. 2019;1(2):507–16. https://doi.org/10.3171/2018.4.JNS18306.
16. Asghari Varzaneh Z, Shanbehzadeh M, Kazemi-Arpanahi H. Prediction of successful aging using ensemble machine learning algorithms. BMC Med Inf Decis Mak. 2022;3(1):258. https://doi.org/10.1186/s12911-022-02001-6.
17. Zhang HW, Wang YR, Hu B, et al. Using machine learning to develop a stacking ensemble learning model for the CT radiomics classification of brain metastases. Sci Rep. 2024;19(1):28575. https://doi.org/10.1038/s41598-024-80210-x.
18. Shen D, Ning C, Huang G, Liu Z. Outcomes of infected pancreatic necrosis complicated with duodenal fistula in the era of minimally invasive techniques. Scand J Gastroenterol. 2019;54(6):766–72. https://doi.org/10.1080/00365521.2019.1619831.
19. Li J, Lin C, Ning C, et al. Early-onset emphysematous pancreatitis indicates poor outcomes in patients with infected pancreatic necrosis. Dig Liver Dis. 2022;54(11):1527–32. https://doi.org/10.1016/j.dld.2022.04.001.
20. Huang H, Peng J, Ning C, et al. Escherichia coli infection indicates favorable outcomes in patients with infected pancreatic necrosis. Front Cell Infect Microbiol. 2023;13:1107326. https://doi.org/10.3389/fcimb.2023.1107326.
21. Mathew G, Agha R, Albrecht J, et al. STROCSS 2021: strengthening the reporting of cohort, cross-sectional and case-control studies in surgery. Int J Surg. 2021;96:106165. https://doi.org/10.1016/j.ijsu.2021.106165.
22. Banks P, Bollen T, Dervenis C, et al. Classification of acute pancreatitis–2012: revision of the Atlanta classification and definitions by international consensus. Gut. 2013;62(1):102–11. https://doi.org/10.1136/gutjnl-2012-302779.
23. Baron TH, DiMaio CJ, Wang AY, Morgan KA. American gastroenterological association clinical practice update: management of pancreatic necrosis. Gastroenterology. 2020;158(1):67–e751. https://doi.org/10.1053/j.gastro.2019.07.064.
24. Working Group IAPAPAAPG. IAP/APA evidence-based guidelines for the management of acute pancreatitis. Pancreatology Jul-Aug. 2013;13(4 Suppl 2):e1–15. https://doi.org/10.1016/j.pan.2013.07.063.
25. Italian Association for the Study of the P, Pezzilli R, Zerbi A, et al. Consensus guidelines on severe acute pancreatitis. Dig Liver Dis. 2015;47(7):532–43. https://doi.org/10.1016/j.dld.2015.03.022.
26. Crockett SD, Wani S, Gardner TB, Falck-Ytter Y, Barkun AN, American Gastroenterological Association Institute Clinical Guidelines C. American gastroenterological association Institute guideline on initial management of acute pancreatitis. Gastroenterology. 2018;154(4):1096–101. https://doi.org/10.1053/j.gastro.2018.01.032.
27. Shen D, Wang D, Ning C, et al. Prognostic factors of critical acute pancreatitis: A prospective cohort study. Dig Liver Dis. 2019;51(11):1580–5. https://doi.org/10.1016/j.dld.2019.04.007.
28. Ning C, Sun Z, Shen D et al. Is Contemporary Open Pancreatic Necrosectomy Still Useful In The Minimally Invasive Era? Surgery. 2024;175(5):1394–1401. https://doi.org/10.1016/j.surg.2024.01.021
29. Yi X, Xiao Q, Zeng F, et al. Computed tomography radiomics for predicting pathological grade of renal cell carcinoma. Front Oncol. 2020;10:570396. https://doi.org/10.3389/fonc.2020.570396.
30. Yi X, Liu Y, Zhou B, et al. Incorporating SULF1 polymorphisms in a pretreatment CT-based radiomic model for predicting platinum resistance in ovarian cancer treatment. Biomed Pharmacother. 2021;133:111013. https://doi.org/10.1016/j.biopha.2020.111013.
31. Yi X, Pei Q, Zhang Y, et al. MRI-Based radiomics predicts tumor response to neoadjuvant chemoradiotherapy in locally advanced rectal cancer. Front Oncol. 2019;9:552. https://doi.org/10.3389/fonc.2019.00552.
32. Zhang Z, Yi X, Pei Q, et al. CT radiomics identifying non-responders to neoadjuvant chemoradiotherapy among patients with locally advanced rectal cancer. Cancer Med. 2023;12(3):2463–73. https://doi.org/10.1002/cam4.5086.
33. DeLong ER, DeLong DM, Clarke-Pearson DL. Comparing the areas under two or more correlated receiver operating characteristic curves: a nonparametric approach. Biometrics. 1988;44(3):837–45.
34. Fagan TJ, Letter. Nomogram for bayes's theorem. N Engl J Med. 1975;31(5):257. https://doi.org/10.1056/NEJM197507312930513.
35. Carnovale A, Rabitti PG, Manes G, Esposito P, Pacelli L, Uomo G. Mortality in acute pancreatitis: is it an early or a late event? JOP. 2005;10(5):438–44.
36. van Santvoort HC, Besselink MG, Bakker OJ, et al. A step-up approach or open necrosectomy for necrotizing pancreatitis. N Engl J Med. 2010;22(16):1491–502. https://doi.org/10.1056/NEJMoa0908821.
37. Bakker OJ, van Santvoort HC, van Brunschot S, et al. Endoscopic transgastric vs surgical necrosectomy for infected necrotizing pancreatitis: a randomized trial. JAMA. 2012;14(10):1053–61. https://doi.org/10.1001/jama.2012.276.
38. van Brunschot S, van Grinsven J, van Santvoort HC et al. Endoscopic or surgical step-up approach for infected necrotising pancreatitis: a multicentre randomised trial. Lancet. 2018;391(10115):51–58. https://doi.org/10.1016/S0140-6736(17)32404-2
39. Zhang L, Zhou J, Ke L, et al. Role of heart rate variability in predicting the severity of severe acute pancreatitis. Dig Dis Sci. 2014;59(10):2557–64. https://doi.org/10.1007/s10620-014-3192-5.

40. Li W, Ou L, Fu Y, Chen Y, Yin Q, Song H. Risk factors for concomitant infectious pancreatic necrosis in patients with severe acute pancreatitis: A systematic review and meta-analysis. Clin Res Hepatol Gastroenterol. 2022;46(5):101901. https://doi.org/10.1016/j.clinre.2022.101901.
41. Brand M, Gotz A, Zeman F, et al. Acute necrotizing pancreatitis: laboratory, clinical, and imaging findings as predictors of patient outcome. AJR Am J Roentgenol. 2014;202(6):1215–31. https://doi.org/10.2214/AJR.13.10936.
42. Rau BM, Kemppainen EA, Gumbs AA, et al. Early assessment of pancreatic infections and overall prognosis in severe acute pancreatitis by procalcitonin (PCT): a prospective international multicenter study. Ann Surg. 2007;245(5):745–54. https://doi.org/10.1097/01.sla.0000252443.22360.46.
43. Liu ZY, Jiang HZ, Wang L, Chen MX, Wang HT, Zhang JX. Diagnostic accuracy of red blood cell distribution width for neonatal sepsis. Minerva Pediatr (Torino). 2022;74(2):202–12. https://doi.org/10.23736/S2724-5276.21.06149-1.
44. Zhang FX, Li ZL, Zhang ZD, Ma XC. Prognostic value of red blood cell distribution width for severe acute pancreatitis. World J Gastroenterol. 2019;28(32):4739–48. https://doi.org/10.3748/wjg.v25.i32.4739.
45. Tokur ME, Korkmaz P, Alkan S, et al. Mortality predictors on the day of healthcare-associated acinetobacter Baumanni bacteremia in intensive care unit. J Infect Dev Ctries. 2022;30(9):1473–81. https://doi.org/10.3855/jidc.16902.
46. Papachristou GI, Muddana V, Yadav D, et al. Comparison of BISAP, ranson's, APACHE-II, and CTSI scores in predicting organ failure, complications, and mortality in acute pancreatitis. Am J Gastroenterol. 2010;105(2):435–41. https://doi.org/10.1038/ajg.2009.622. quiz 442.
47. Lu J, Ding Y, Qu Y, et al. Risk factors and outcomes of Multidrug-Resistant bacteria infection in infected pancreatic necrosis patients. Infect Drug Resist. 2022;15:7095–106. https://doi.org/10.2147/IDR.S387384.
48. Ding L, Yu C, Deng F, et al. New risk factors for infected pancreatic necrosis secondary to severe acute pancreatitis: the role of initial Contrast-Enhanced computed tomography. Dig Dis Sci. 2019;64(2):553–60. https://doi.org/10.1007/s10620-018-5359-y.
49. Pamies-Guilabert J, Del Val Antonana A, Collado JJ, Rudenko P, Meseguer A. Pancreatic necrosis volume - A new imaging biomarker of acute pancreatitis severity. Eur J Radiol. 2020;130:109193. https://doi.org/10.1016/j.ejrad.2020.109193.
50. Li XY, He C, Zhu Y, Lu NH. Role of gut microbiota on intestinal barrier function in acute pancreatitis. World J Gastroenterol. 2020;14(18):2187–93. https://doi.org/10.3748/wjg.v26.i18.2187.
51. Foitzik T, Stufler M, Hotz HG, et al. Glutamine stabilizes intestinal permeability and reduces pancreatic infection in acute experimental pancreatitis. J Gastrointest Surg Jan-Feb. 1997;1(1):40–6. https://doi.org/10.1007/s11605-006-0008-8. discussion 46– 7.
52. Huang L, Zhang D, Han W, Guo C. High-mobility group box-1 Inhibition stabilizes intestinal permeability through tight junctions in experimental acute necrotizing pancreatitis. Inflamm Res. 2019;68(8):677–89. https://doi.org/10.1007/s00011-019-01251-x.
53. Mao W, Li K, Zhou J, et al. Prediction of infected pancreatic necrosis in acute necrotizing pancreatitis by the modified pancreatitis activity scoring system. United Eur Gastroenterol J. 2023;11(1):69–78. https://doi.org/10.1002/ueg2.12353.
54. Lan L, Guo Q, Zhang Z, et al. Classification of infected necrotizing pancreatitis for surgery within or beyond 4 weeks using machine learning. Front Bioeng Biotechnol. 2020;8:541. https://doi.org/10.3389/fbioe.2020.00541.
55. Westcott A, Capaldi DPI, McCormack DG, Ward AD, Fenster A, Parraga G. Chronic obstructive pulmonary disease: thoracic CT texture analysis and machine learning to predict pulmonary ventilation. Radiology. 2019;293(3):676–84. https://doi.org/10.1148/radiol.2019190450.
56. Ma Y, Ji J, Huang Y, et al. Implementing machine learning in bipolar diagnosis in China. Transl Psychiatry. 2019;18(1):305. https://doi.org/10.1038/s41398-019-0638-8.

Publisher's note